Microfluid Nanofluid (2006) 2: 89–96
DOI 10.1007/s10404-005-0048-5

RESEARCH PAPER

S. Messner · J. Schaible · H. Sandmaier · R. Zengerle

3-way silicon microvalve for pneumatic applications with electrostatic actuation principle

Received: 12 February 2005 / Accepted: 18 May 2005 / Published online: 28 July 2005

Abstract We present a normally closed electrostatically driven 3-way microvalve which is able to meet the requirements of industrial applications like small form factor, high flow rate, low weight, low power consumption and a short response time. The microvalve consists of a 3 layer full-wafer bonded silicon chip stack mounted on a ceramics substrate and a plastic cap covering the valve. A driver electronics which converts the TTL level to the actuation voltage of 200 V is placed on top of the valve. The valve operates in a pressure range of up to 8 bar and offers a flow rate of approximately 500 sccm. Due to the electrostatic actuation principle the peak power consumption is below 10 mW and the response time is below 1 ms.

Keywords Microvalve · Electrostatic actuation · Silicon micromachining · Pneumatics

1 Introduction

In many industrial fields, especially in automation, there is a trend towards decentralization and intelligent, stand-alone operating sub systems. A pneumatic cylinder containing microvalves, sensors and control electronics could be such a sub system which is able to carry out commands independently and perform self diagnostics. Ideally such a cylinder only needs the pneumatic interfaces for the pressurized air and an electronic interface for information exchange, but no additional interface for electrical power. This trend leads to the need of miniaturized components with low power consumption meeting the requirements for industrial applications. Microvalves for industrial, pneumatic applications must have a 3-way normally closed functionality, a high air flow, a low leakage rate, a short response time, a wide temperature range (−40 to 80°C) and have to operate in the standard pressure range of 0–8 bar (8×10^5 Pa). To work in sub systems with the power provided, for example by serial interfaces, the power consumption has to be as low as possible. To enable the integration in sub systems like pneumatic cylinders, the outer dimensions of the valve have to be as small as possible. Ideally the form factor should be compatible with standard pneumatics, where the width of the valves is standardized and 10 mm is the smallest standard at present.

In the past several microvalves with different actuation principles were presented [1–8]. All of these valves show very good properties for special applications, but up until now there is no microvalve which meets all the requirements mentioned above. A very important requirement for pneumatic applications is the 3-way normally closed functionality of the valve. Besides the inlet and outlet port, 3-way valves embody a third port, the exhaust. The inlet port is connected to the pressure supply, and the outlet port is connected to the consumer (e.g. a pneumatic cylinder). The exhaust is connected to ambience. In the basic, not actuated state the inlet port of normally closed 3-way valves is blocked and the outlet is connected to the exhaust. In the actuated state the pressure (inlet port) is connected to the outlet port while the port to ambience is blocked. By switching between these two states the pressure at the outlet can be switched between the supply pressure and ambient

S. Messner (✉) · R. Zengerle
HSG-IMIT, Wilhelm-Schickard-Str. 10
78052 Villingen-Schwenningen, Germany
E-mail: stephan.messner@hsg-imit.de
Tel.: +49-7721-943243
Fax: +49-7721-943210

J. Schaible
Hoerbiger-Origa Systems GmbH, Südliche Römerstrasse 15
86972 Altenstadt, Germany

R. Zengerle
IMTEK, University of Freiburg, Georges-Köhler-Allee 103
79110 Freiburg, Germany

H. Sandmaier
IFF-LMST, University of Stuttgart, Nobelstraße 12
70569 Stuttgart, Germany

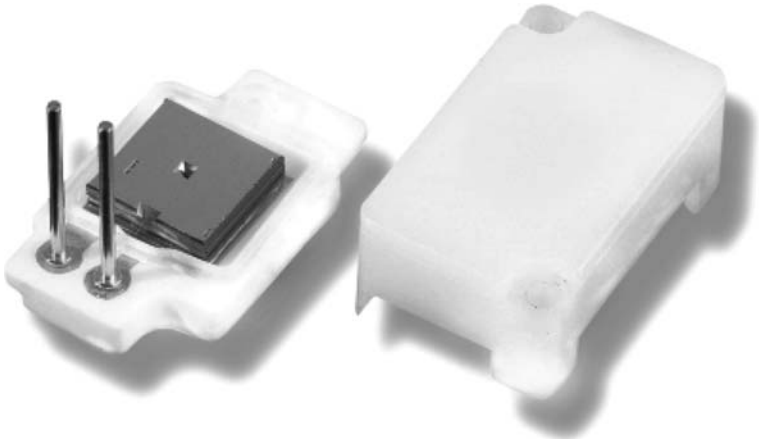

Fig. 1 Photograph of the microvalve with removed plastic cap

pressure which enables pneumatic work to be performed at the outlet port (e.g. move a pneumatic cylinder).

The electrostatically driven microvalve that we present is the first normally closed 3-way electrostatically driven microvalve. Figure 1 shows a photograph of the microvalve with the plastic cap removed.

2 Design and layout

The design of the 3-way microvalve is an advancement of the 2-way design that was presented earlier [9]. Figure 2 shows a cross-section of the 3-way silicon microvalve chip fabricated by silicon micromachining.

The silicon microvalve itself consists of three layers. The bottom chip contains the outlet and the exhaust port. The movable valve plate is part of the plate chip and the cover chip contains the pressure (inlet) port. In order to realize a normally closed valve function the pressure port must be sealed against the inlet pressure of up to 8 bar (8×10^5 Pa) in the not actuated state of the valve. This is done by pre-stressing the valve plate. The valve seat of the pressure port is raised by a few micrometers (z_p) with reference to the outer area of the chip. This is realized by wet chemically etching the outer area of the chip. When mounting the cover chip to the plate chip the raised area leads to a deflection of the valve plate and thus to a pre-stressed valve plate suspension which works as a spring.

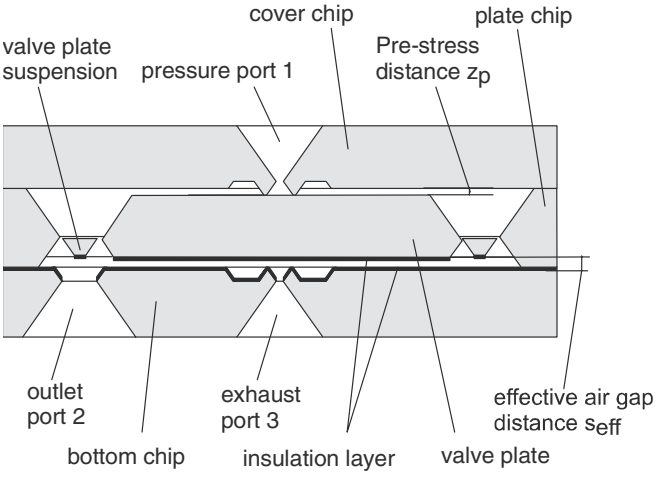

Fig. 2 Cross-sectional, schematic view of the silicon microvalve

The normally closed function is guaranteed when the resulting force of the pre-stressed suspension is higher than the force resulting from the inlet pressure.

The electrostatic actuation principle was chosen for its low power consumption, independency on the ambient temperature, fast response time and unique possibility for integration within silicon bulk micromachining. By applying a voltage between the bottom and plate chip, an electrostatic field is generated in the air gap between the valve plate and bottom chip. The resulting electrostatic force moves the valve plate towards the bottom chip. An insulation layer prevents short circuits. The deflection of the valve plate leads to a resulting force of the valve plate suspension which works against the electrostatic force. Figure 3 shows a schematic drawing of the plate chip.

The valve plate is suspended on four elastic beams that are trapezium shaped. The reset force of the valve plate suspension can be calculated as follows:

$$F_{\mathrm{res}} = kz, \tag{1}$$

where z is the actual deflection of the valve plate and k is the stiffness (spring constant) of the suspensions. For a small deflection of the beam, which is less than 5% of its thickness, a linear spring constant can be assumed. For the trapezium shape it can be calculated according to the following equation:

$$k = \frac{4}{3}\left(\frac{E}{1-\nu^2}\right)\frac{\left(b_1^2 + 4b_1b_2 + b_2^2\right)h^3}{(b_1+b_2)l^3} \tag{2}$$

where E is the Young's modulus and ν is Poisson's ratio. The geometrical parameters b_1, b_2, h and l are the geometrical dimensions of the trapezium shaped elastic beams and are shown in Fig. 3.

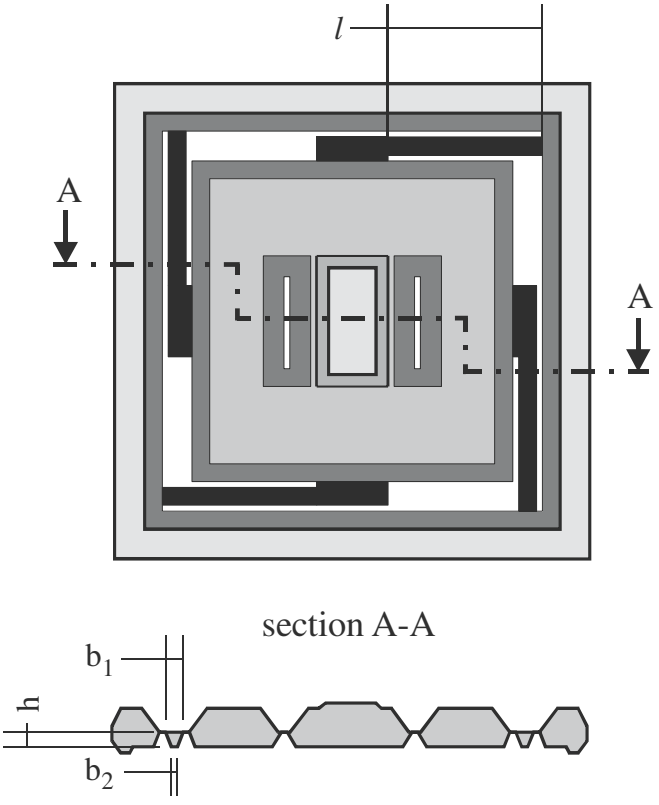

Fig. 3 Schematical drawing of the plate chip

The electrostatic force, induced by the applied electrical field, can be calculated using the following equation:

$$F_{\mathrm{elst}} = \frac{1}{2}\left(\frac{\varepsilon_0}{\kappa_{\mathrm{air}}}\right) A_{\mathrm{el}} U_{\mathrm{e}}^2 \left[\frac{1}{\left(\frac{d_{\mathrm{in}}}{\kappa_{\mathrm{in}}} + \frac{s-z}{\kappa_{\mathrm{air}}}\right)^2}\right] \tag{3}$$

where ε_0 is the permittivity, κ_{air} and κ_{in} are the dielectric constants for air and the insulation layer. A_{el} is the electrostatically active surface, U_{e} is the voltage applied, d_{in} is the thickness of the insulation layers and s is the initial air gap height. The equilibrium of the mechanical reset force (Eq. 1) and the electrostatic actuation force (Eq. 3) considering Eq. 2 leads to the following equation where $s_{\mathrm{eff}} = s + d_{\mathrm{in}}/\kappa_{\mathrm{in}}$ is the effective air gap distance between the electrodes (valve plate/bottom chip) and it is assumed that $\kappa_{\mathrm{air}} = 1$.

$$z^3 - 2s_{\mathrm{eff}}z^2 + s_{\mathrm{eff}}^2 z - \frac{1}{2}\left(\frac{\varepsilon_0 A_{\mathrm{el}}}{k}\right) U_{\mathrm{e}}^2 = 0 \tag{4}$$

This equation describes the deflection of the valve plate depending on the electrical voltage applied. In the range $0 \le z/s_{\mathrm{eff}} < 1/3$ the deflection z of the valve plate is stable; for $z/s_{\mathrm{eff}} \ge 1/3$ the deflection is unstable [10] and the valve plate snaps down to the bottom chip and seals the exhaust. The solution of the cubic Eq. 4 leads to the switching voltage where the deflection gets unstable of:

$$U_S = \sqrt{\frac{8}{27}\left(\frac{k s_{\mathrm{eff}}^3}{\varepsilon_0 A_{\mathrm{el}}}\right)} \tag{5}$$

In the case of the design presented in Fig. 2 the prestress distance z_{p} has to be considered which leads to Eq. 6.

$$U_S = \sqrt{\frac{8}{27}\left[\frac{k(s_{\mathrm{eff}} + z_p)^3}{\varepsilon_0 A_{\mathrm{el}}}\right]} \tag{6}$$

If the voltage applied to the microvalve is higher than U_{s}, the valve plate snaps down to the bottom chip and seals the exhaust. To keep the switching voltage within a reasonable range below 200 V the air gap distance has to be less than 5 μm, considering that k is 50 kN/m, A_{el} is 15 mm^2 and z_{p} is 2 μm.

The force induced by the pneumatic pressure is not considered in Eq. 1 because it acts in the same direction as the electrostatic force and leads to a reduced switching voltage. Thus, in terms of the switching voltage Eq. 1 represents the worst case when no pressure is applied to the valve. Consequently, the valve plate suspensions have to be weak enough so that the relatively low electrostatic force is sufficient to deflect the valve plate. On the other hand, when the maximum pressure of 8 bar (8×10^5 Pa) is applied and the electrostatic field is absent, the valve plate suspensions have to be stiff enough to move the valve plate back.

To minimize the forces induced by the pneumatic pressure on the valve plate, the valve is designed in a way so that the pressure difference between the inlet and outlet only works on the small area within the valve seat area. Thus, a high pneumatic pressure can be controlled using a relatively small electrostatic force.

The flow rate of the valve is mainly influenced by the highest flow resistance in the valve which is in the area of the valve seats and is determined by the smallest cross-section for the air flow. Taking a very small air gap distance into account the smallest cross-section for the flow is determined by the perimeter length of the valve seat multiplied with the air gap distance. To achieve a maximum flow rate, the perimeter length of the valve seat has to be as long as possible, however, ensuring that the enclosed area of the valve seat is as small as possible. This approach to increase the flow rate of the microvalves was already earlier presented in [11–14]. One method to increase the perimeter length while considering that the enclosed surface is a constant is to use a meandered valve seat as presented in [9] and [15]. Another method to optimize the flow rate of microvalves is to use multiple orifices and thus to increase the ratio of the perimeter length to the enclosed area of the valve seat. This approach was presented in [16, 17] and [18] and could be used for further optimization of the microvalve presented here.

To be able to estimate the flow rate of the microvalve by analytical means, some assumptions and

Table 1 List of parameters for the calculation of the volume flow

Parameter	p'_1 [Pa]	p'_2, p'_s [Pa]	A_M [m^2]	μ_m [1]	γ [1]	R [J/Kg·K]	T_s [K]
Value	7×10^5	1.013×10^5	1.125×10^{-8}	0.6	1.4	287	293.15

simplifications are necessary. It is assumed that the velocity of the inflowing gas is negligible compared to the velocity at the smallest cross-section (nozzle). Thus, a steady state expansion flow can be presumed.

Furthermore it is assumed that the change of state is isentropic. After [19], these assumptions lead to the following Eq. 7:

$$\dot{m}_{\mathrm{th}} = \mu_M A_M \Psi_{A,2} \sqrt{2\left(\frac{p'_1}{v_1}\right)} \tag{7}$$

This equation describes the mass flow through a nozzle, where μ_M is an empirically determined factor taking into account the friction and the shape of the nozzle. A_M is the area of the smallest cross-section (nozzle). The absolute pressure at the inlet of the valve is p'_1 and $v_1 = 1/\rho_1$ is the reciprocal value of the gas density at the inlet of the valve. $\Psi_{A,2}$ is a nondimensional term and calculated from the following equation:

$$\Psi_{A,2} = \sqrt{\frac{\gamma}{\gamma-1}\left[\left(\frac{p'_2}{p'_1}\right)^{\frac{2}{\gamma}} - \left(\frac{p'_2}{p'_1}\right)^{\frac{\gamma+1}{\gamma}}\right]} \tag{8}$$

$\Psi_{A,2}$ only depends on the ratio between the absolute pressure at the outlet p'_2 and the absolute pressure at the inlet p'_1, and the adiabatic exponent γ which is the ratio of specific heats c_p/c_v depends on the type of gas ($\gamma = 1.4$ for air). $\Psi_{A,2}$ has a parabolic shape commencing at $\Psi_{A,2} = 0$ for a pressure ratio $p'_2/p'_1 = 1$. If the pressure ratio decreases, $\Psi_{A,2}$ increases up to its maximum

$$\Psi_{A,\max} = \left(\frac{2}{\gamma+1}\right)^{\frac{1}{\gamma-1}} \sqrt{\frac{\gamma}{\gamma+1}} \tag{9}$$

at the Laval (or critical) pressure ratio of:

$$P_{kr} \equiv P_L = \left(\frac{2}{\gamma+1}\right)^{\frac{\gamma}{\gamma-1}} \tag{10}$$

If the pressure ratio decreases further, $\Psi_{A,2}$ and thus the mass flow through the nozzle remains a constant.

For pneumatic valves the volume flow $\dot{V}$ is used to specify the flow characteristic of valves. Since it depends on the actual pressure, the temperature and the density of the medium the volume flow with reference to standard conditions (p'_s, T_s see Table 1) is used. The standard volume flow (standard flow rate) $\dot{V}_s$ can be calculated using the following equation:

$$\dot{V}_s = \frac{\dot{m}}{\rho_s} = \left(\frac{RT_s}{p'_s}\right)\dot{m} \tag{11}$$

The mass flow through the nozzle is the same at each position (before and behind). The standard flow rate depends on the density ρ_s, the gas constant R, the temperature T_s and the absolute pressure p'_s. Using Eq. 11 the standard volume flow through the microvalve can be calculated to be $\dot{V}_s = 556$ sccm (standard cubic centimeters per minute) considering the parameters listed in table1.

The area of the smallest cross-section (nozzle) A_M in Table 1 is calculated by the perimeter length of the valve seat $P_v = 3.75\times10^{-3}$ m multiplied with the air gap distance $s = 3\times10^{-6}$ m. The calculated volume flow rate is valid for the flow from the pressure port to the outlet port in the actuated state of the valve as well as for the flow from the outlet port to the exhaust in the not actuated state of the valve. In this calculation only the biggest flow resistance in the area of the valve seat is taken into account. Further flow resistances are considered negligible. Also, the reduction of the air gap distance as a consequence of the inlet pressure respectively a warpage of the cover chip is not considered in the calculation. Taking these simplifications into account, the measured flow rate should be smaller than the calculated value.

3 Fabrication

The actual microvalve is manufactured by silicon bulk micromachining. The three silicon layers are structured separately by wet and dry etching technologies. After structuring, the bottom wafer and the plate wafer are coated with an insulation layer (silicon dioxide) which is also used as the bonding layer for the silicon fusion bonding process to mount the three layers together. In order to prevent bonding between the valve plates of the plate wafer and the raised (see above) pressure port 1 seats of the cover wafer, the seats are coated with a layer which prevents bonding. The silicon dioxide and nitride passivation layers used for the structuring of pressure port 1 seats are not removed after structuring of the cover wafer and act as the layer which prevents bonding. After bonding, the wafer stack is diced into single valve chips. A more detailed description of the fabrication process is presented in [20].

Figure 4 shows the packaging concept. The silicon valve chip is mounted to a ceramic substrate which contains two metal pads prepared by screen printing. The bottom chip of the valve is connected to the first pad using an electrically conductive adhesive. The plate chip is connected to the second pad by wire bonding. The two pads are connected to the contact pins also using the electrically conductive adhesive. The contact pins are used as the external electrical interface to the valve.

All three pneumatic ports are at the bottom side of the ceramics substrate. The outlet and exhaust port of the ceramics substrate are directly connected to the

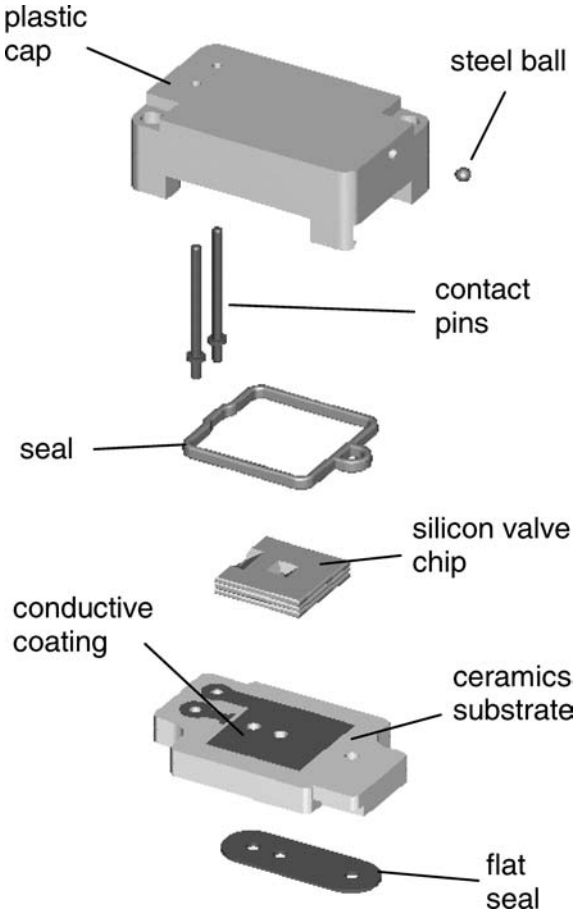

Fig. 4 Packaging concept of the microvalve

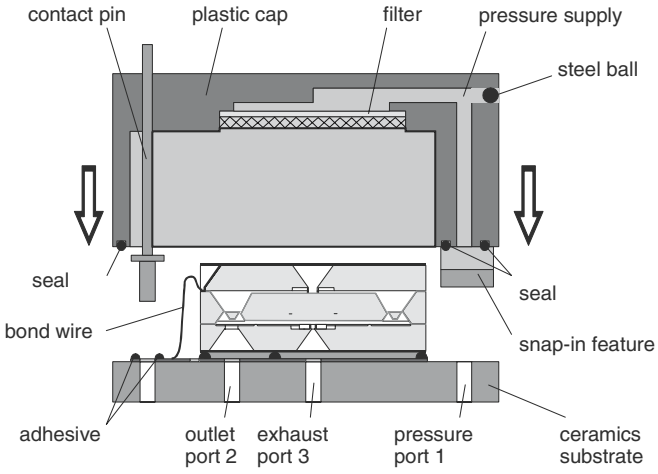

Fig. 5 Cross-sectional view of the microvalve assembly

outlet and exhaust of the silicon valve chip. The seal is realized by the gluing process. The pressure port of the ceramics substrate is connected to a small channel inside the plastic cap which conducts the pressure through a particle filter to the top side of the valve (Fig. 5).

The plastic cap is mounted to the ceramics substrate using snap-in features. A seal between ceramics substrate and plastic cap prevents leakage. The completely assembled microvalve can be mounted onto an adapter block using screws. A flat seal between valve and adapter block prevents leakage and "cross-talk" between the different ports. The outer dimensions of the valve chip are 6×6×1.5 mm^3, the outer dimensions of the packaged valve are 16×10×7 mm^3.

A driver electronics which converts a 3 V input voltage into 200 V output voltage is placed on top of the microvalve. The overall power consumption is approximately 10 mW. Figure 6 shows the completely assembled microvalve with the unpackaged driver electronics on top.

4 Measurement results

To characterize a 3-way valve different measurements have to be carried out. The pressure values p_1, p_2 and p_3 used in the following are relative pressure values.

Figure 7 shows the typical flow rate from the pressure port to the outlet port.

Four different valves of the same type were measured. Due to the high quality full-wafer-bond only small variations occur between the different valves of the same type. The principle setup used for this measurement is shown in Fig. 8.

The measurements were taken, with a voltage of U_e = 200 V applied to the valve. In this state the exhaust port is blocked by the valve plate and air flows from the pressure port to the outlet port. Outlet port and exhaust port are connected to ambient pressure. The

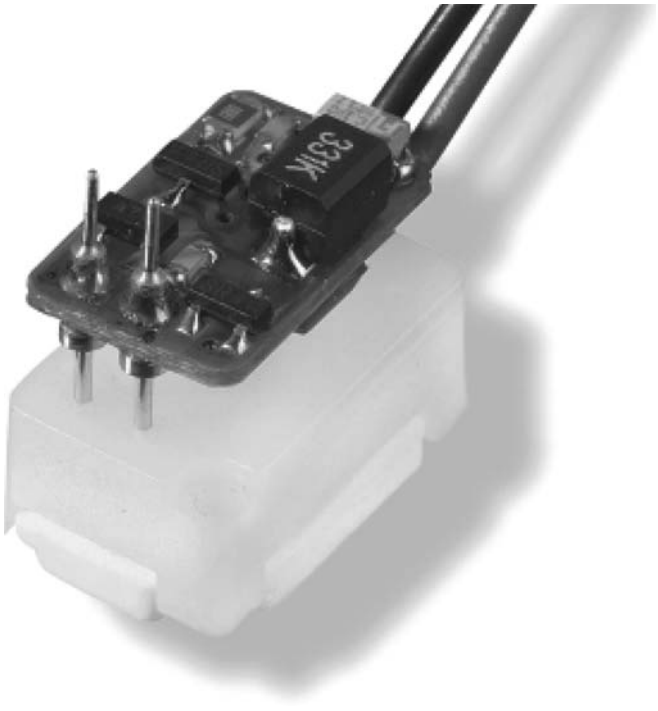

Fig. 6 Completely assembled 3-way microvalve with driver electronics mounted on top

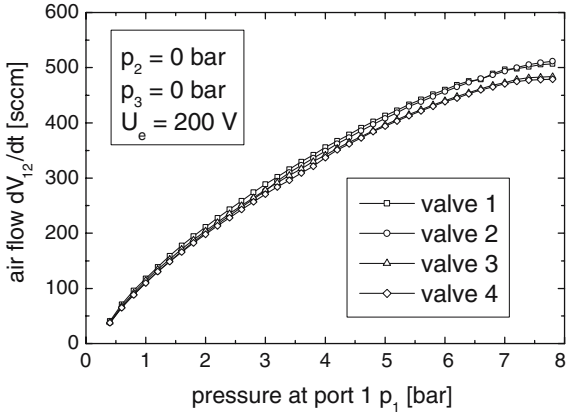

Fig. 7 Measured flow rate from pressure to outlet port versus pressure at pressure port (1 bar = 10^5 Pa)

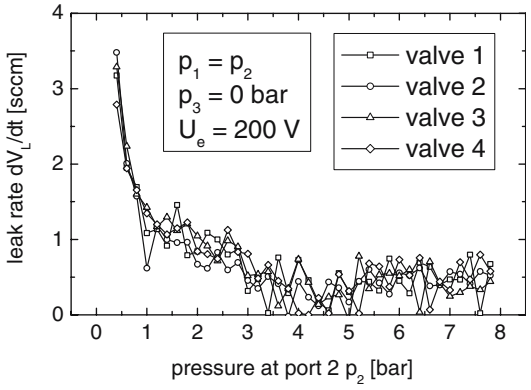

Fig. 9 Leak rate at exhaust versus pressure at outlet port 2 (1 bar = 10^5 Pa)

flow rate is measured at the outlet port. At a pressure difference of 6 bar (6×10^5 Pa), which is the standard pressure for pneumatic applications, the air flow is approximately 475 sccm.

In Fig. 9 the leak rate at the exhaust port for the above mentioned state of the valve is shown. The setup for this measurement is shown in Fig. 10. At a pressure difference of 6 bar the leak rate is below 1 sccm which is approximately 0.2% of the maximum flow rate. For low pressures the leak rate increases. The reason for this is, that the applied pressure leads to a force on the valve plate and supports the sealing at the valve seat of the exhaust port. Thus, if the pressure gets higher, the force on the valve plate increases and the sealing is better.

In the basic state of the valve, with no voltage applied, the pressure port is blocked by the valve plate. The air flows from the outlet port to the exhaust port where the air flow is measured. To perform this measurement, the pressure is simultaneously applied to the outlet port and pressure port. Figure 10 in principle shows this measurement setup. The only difference is that the applied voltage is $U_e = 0$ V. The maximum flow rates for the four measured valves vary between 350 and 450 sccm (see Fig. 11). The flow rate decreases for pressures above 6 bar, contrary to what normally would be expected. The reason for this is the pressure difference between inside and outside the silicon microvalve which causes a warpage of the cover chip and thus a reduction of the air gap distance at the valve seat and consequently a decrease in flow rate. The pressure inside the silicon microvalve is lower than the applied pressure, because of internal flow resistances.

Figure 12 shows the typical hysteresis of the electrostatic actuation principle. The air flow from the pressure port to the outlet port versus the applied voltage is shown. The setup shown in Fig. 8 is used for this investigation. When no voltage is applied the valve plate seals the pressure port. At the switching voltage $U_{s,1}$ of about 60 V the valve plate snaps in its second stable position and seals the exhaust port. The air flow from inlet port to outlet port is approx. 475 sccm. The voltage $U_{s,2}$ where the valve plate moves back in its original position is lower, because the effective distance s_{eff} between the electrodes is lower than in the original position. Thus the electrostatic force at a given voltage is higher.

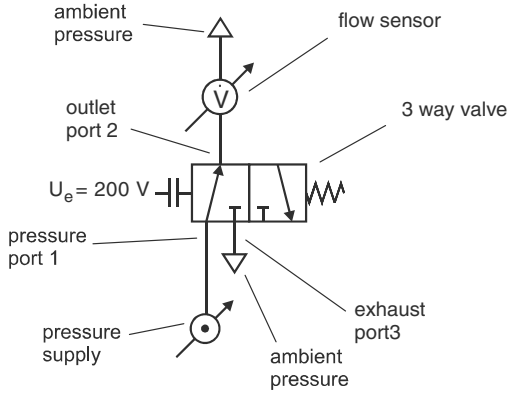

Fig. 8 Setup for the measurement of the flow rate from pressure port 1 to outlet port 2

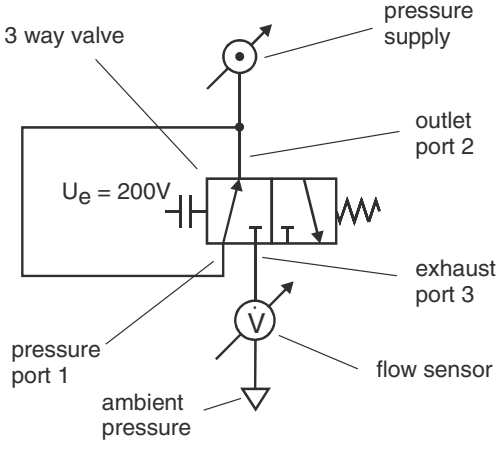

Fig. 10 Setup for the measurement of the leak rate to the exhaust port 3

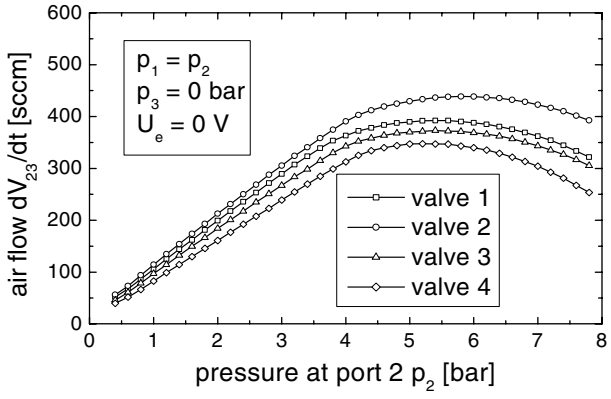

Fig. 11 Measured flow rate from outlet to exhaust port versus pressure at outlet port (1 bar = 10^5 Pa)

The switching voltage $U_{s,1}$ depends on the inlet pressure, because the inlet pressure induces a force to the valve plate. Figure 13 shows the mean values of $U_{s,1}$ and $U_{s,2}$ versus the pressure at the pressure port of the four measured valves. The variations in the measurement results are caused by fabrication tolerances and the measurement accuracy. The pressure dependence of the switching voltage $U_{s,1}$ can clearly be seen. Against simple approximations $U_{s,2}$ is also depending on the inlet pressure. The pressure difference between inside and outside of the silicon microvalve causes a deformation which leads to a change in the effective distance of the electrodes and thus to a change in $U_{s,2}$. Electrostatic charging of the dielectric, which occurs during operation of the valve and leads to a change in the switching voltage, is a known problem for electrostatic micro actuation units [21]. To prevent this effect, the driver electronics was designed in a way, that the polarity of the output voltage is reversed at regular intervals.

In Figure 14 the mechanical response time of the valve plate is shown. The movement of the valve plate was measured by using an optical distance sensor. For this measurement, the cover chip was removed from the valve to provide access to the valve plate. This investigation was carried out at atmospheric pressure. By applying 200 V between bottom and plate chip the valve plate moves within less than 0.5 ms.

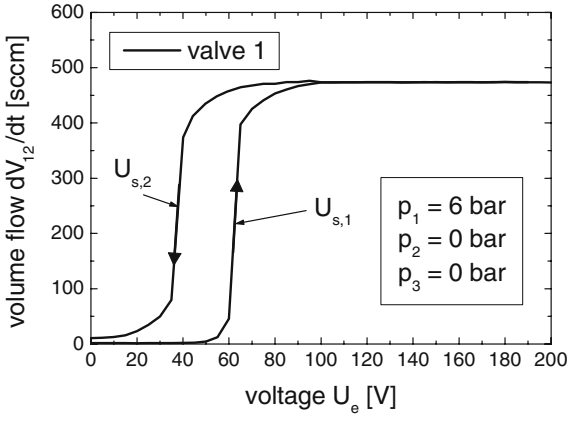

Fig. 12 Flow rate from pressure to outlet port versus applied voltage (1 bar = 10^5 Pa)

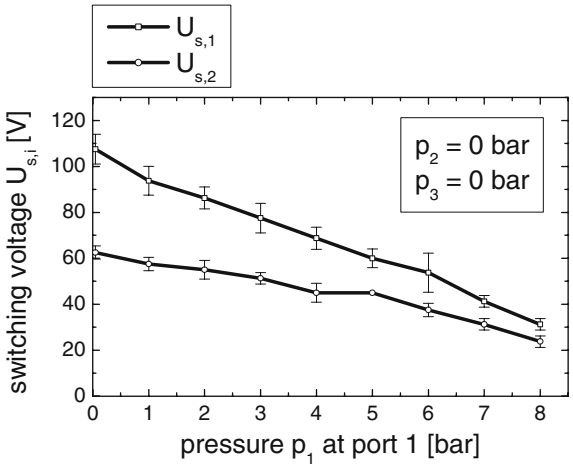

Fig. 13 Switching voltages $U_{s,1}$ and $U_{s,2}$ versus pressure at pressure port 1 (1 bar = 10^5 Pa)

5 Conclusion

We presented a normally closed 3-way silicon microvalve meeting industrial requirements such as small size, fast switching times and low power consumption. It was shown that this valve is able to control the required pressure of 6 bar which is used as a standard in industry. The overall power consumption of the valve is less than 10 mW, enabling the control of the valve simply by logical signals (3–5 V, ∽2 mA) without an additional power supply.

The valve chips were completely fabricated using silicon micromachining. The 3 layer wafer stack was bonded by two successive silicon fusion bonds with one of them generating a pre-stress to the valve plate in order to seal the pressure port against a pneumatic pressure of

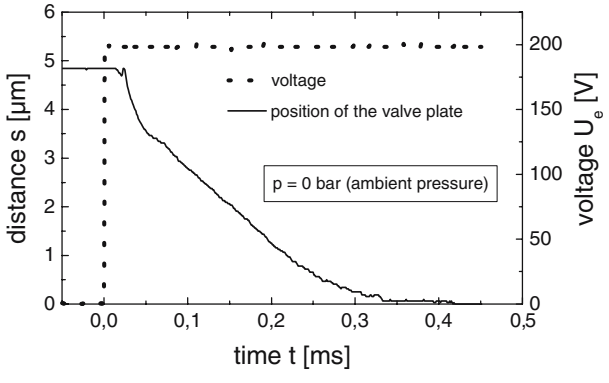

Fig. 14 Mechanical response time of the valve plate

up to 8 bar (8×10^5 Pa). It can be seen from Figs. 7, 9, 11 and 13 that the fabrication on full wafer level results in a very good homogeneity of the manufactured valves. Further work will be carried out to optimize the valve with regards to series production.

Acknowledgements The authors would like to thank the State of Baden-Württemberg (Germany) for the financial support of this research.

References

1. Jerman JH (1991) Electrically-activated, normally closed diaphragm valves. In: Proceedings transducers 91, IEEE, Picataway, NJ, USA, pp 1045–1048
2. Zdeblick MJ, Anderson R, Jankowski J, Kline-Schoder B, Christel L, Miles R, Weber M (1994) Thermopneumatically actuated microvalve and integrated electro-fluidic circuits. In: Proceedings actuator 94, Axon Technologie Consult GmbH, Bremen, Germany, pp 56–60
3. Ohnstein T, Fukiura T, Ridley J, Bonne U (1990) Micromachined silicon microvalve. In: Proceedings IEEE MEMS 90, IEEE, Piscataway, NJ, USA, pp 95–98
4. Messner S, Muller M, Burger V, Schaible J (1998) A normally closed, bimetallically actuated 3-way microvalve for pneumatic applications. In: Proceedings IEEE MEMS 98, IEEE, Piscataway, NJ, USA, pp 40–44
5. Huff MA, Gilbert JR, Schmidt MA (1993) Flow characteristics of a pressure-balanced microvalve. In: Proceedings transducers 93, IEEE, Piscataway, NJ, USA, pp 98–101
6. Shikida M, Sato K (1994) Electrostatically driven gas valve with high conductance. J Microelectromech Syst. IEEE/ASME Publication; Belle Mead, USA, 3(2):76–80
7. Barth PW, Beatty CC, Field LA, Baker JW, Gordon GB (1994) A robust normally closed silicon microvalve. In: technical digest solid-state sensor and actuator workshop, Transducers Research Foundation, Cleveland, OH, USA, pp 248–250
8. Tsai M-J, Hsu S-C, Ke C-H, Jang R-H, Wu C-Y (1998) A thermally buckling microvalve with integrated flow sensor. In: Proceedings actuator 98, Messe Bremen GmbH, Bremen, Germany, pp 130–136
9. Schaible J, Vollmer J, Zengerle R, Sandmaier H, Strobelt T (2001) Electrostatic microvalves in silicon with 2-way-function for industrial applications. In: Proceedings transducers 2001, Springer, Berlin Heidelberg New York
10. Gupta RK (1997) Electrostatic pull-in test structure design for in-situ mechanical property measurements of microelectromechanical systems (MEMS). PhD Thesis, Massachusetts Institute of Technology, Cambridge, USA
11. Wang T, Barth P, Alley R, Baker J, Yates D, Field L, Gordon G, Beatty C, Tully L (1999) Production-ready silicon microvalves. SPIE proceedings, vol 3876. SPIE, Bellingham, pp 227–237
12. Henning AK (2003) Improved gas flow model for microvalves. In: Proceedings, Transducers 2003, IEEE Press, Piscataway, NJ, USA, pp 1550–1553
13. Henning AK (2004) Confirmation of large periphery compressible gas flow model for microvalves. In: SPIE proceedings, vol 5344. SPIE, Bellingham, pp 155–162
14. Zengerle R, Wirtl J, Frisch H (1997) Mikroventil. German patent DE19546181
15. Schaible J (2001) Mikrotechnisch hergestellte Schaltventile für Gase. PhD Thesis, University of Stuttgart, Germany
16. van der Wijngaart W, Thorsén A, Stemme G (2004) A seat microvalve nozzle for optimal gas flow capacity at large controlled pressure. In: Proceedings IEEE MEMS 2004, IEEE, Piscataway, NJ, USA, pp 233–236
17. Aine H, Block B (1986) Miniature valve and method of making same. US patent US4585209
18. Richter M, Kluge S (1998) Microvalve. European patent EP0836012
19. Sigloch H (1991) Technische Fluidmechanik. VDI Verlag, Düsseldorf, Germany
20. Messner S (2000) Elektrostatisch angetriebenes 3/2-Wege-Mikroventil für pneumatische Anwendungen. PhD Thesis, Albert-Ludwigs-University Freiburg, Germany
21. Wibbeler J, Pfeiffer G, Hietschold M (1998) Parasitic charging of dielectric surfaces in capacitive microelectromechanical systems (MEMS). Sensors and Actuators A, Elsevier, The Netherlands, 71:74–80